2-D digital curve analysis : a regularity measure

Bruno Vasselle, Gerard Giraudon

INRIA

INSTITUT NATIONAL DE RECHERCHE EN INFORMATIQUE ET EN AUTOMATIQUE

2-D digital curve analysis : A regularity measure

Bruno VASSELLE
Gérard GIRAUDON

N° 1915
Mai 1993

PROGRAMME 4

Robotique, image
et
vision

Rapport de recherche

1993

2-D Digital Curve Analysis : A Regularity Measure

Analyse de Courbe Discrète 2-D : Proposition d'une Mesure de Régularité

Bruno VASSELLE and Gérard GIRAUDON

INRIA 2004 Route des Lucioles - Sophia Antipolis

0650 VALBONNE - FRANCE

April 1993

Programme 4: Robotique, Image et Vision

Abstract

Recent experimental results [1] *on human vision show that low fractal dimension curves are highly capable to evocate namable objects. In other terms, regular curves are recognized by human vision as object edges. In this report, a regularity measure of discrete lines geometry is presented. This scalar measure is based on a ratio between lines lengths at different scale. It is analyzed in the framework of brownian motion theory. The measure at a given scale is always computed from the maximum precision image, so that it doesn't introduce any sub-resolution assumption. A scale choice determines the quantity of global information vs. local information one wants to measure. We show how this quantitative measure leads to a relevant shape information. To illustrate this, an image segmentation application example is realized. The segmentation is based essentially on geometry criteria. The segmentation process uses a region growing process which depends on a single parameter that can be fixed in a natural way comparing boundaries regularity to a geometric model regularity. We present experimental results performed on real-scene images, including indoor and outdoor images.*

Résumé

Des récents travaux sur la vision humaine montrent que des courbes ayant une faible dimension fractale suggèrent à la perception humaine des objets familiers. En d'autres termes, les courbes régulières sont reconnues par la vison humaine comme des frontières d'objets. Dans ce rapport, nous présentons une mesure de régularité de courbes géométriques discrètes. Cette mesure scalaire, basée sur le rapport entre les longueurs des lignes à différentes échelles est analysée dans le cadre de la théroie du mouvement brownien. Pour une échelle donnée, la mesure est toujours calculée à la précision maximale de l'image, de sorte que nous n'introduisons pas une quelconque hypothése de sous échantillonage. Le choix d'une échelle détermine la quantité d'information globale ou locale que nous voulons mesurer. Nous montrons comment cette mesure quantitative permet d'obtenir une information pertinente sur la forme elle-même. Pour illustrer ceci, nous présentons un exemple d'utilisation de la mesure dans le cadre de la segmentation d'image. La segmentation qui est essentiellement basée sur un critére géométrique utilise un processus de croissance de régions qui dépend d'un seul paramètre qui peut être fixé de maniére naturelle en comparant la régularité des frontiéres de régions avec la régularité d'un modéle géométrique. Nous présentons des résultats expérimentaux sur des images réelles de scènes d'intérieur et d'extérieur.

[1] Rogowitz and Voss, "Shape Perception and Low-Dimension Fractal Boundary Contours". Research Report, IBM Research Division, July 16, 1990.

1 Introduction

It is a common experience to recognize familiar objects in apparently random shapes such as clouds or mountains. In a recent article, Rogowitz an Voss [1] have presented a series of experimental results which shows that this evocation power is due to contours, and that it is as much important as the fractal dimension of contours is low. For the human perceptual system, regularity of boundaries seems to have a drastic importance.

So it is not surprising that regularity measures are widely used in Computer Vision. For shape classification and recognition, regularity appears in the notion of *critical points*. These points are defined as singularities - we could say *irregularities* - in curve features such as tangent or curvature discontinuities. It appears that most of shape information is supported by these points. For example, Mokhtarian and Mackwoth [2] build a nice shape representation by studying the evolution of null curvature points in the scale space. Asada and Brady [3] study isolated curvature changes such as *corners* or *smooth joints*, and compound changes such as *cracks*, *ends*, *bumps* or *dents*. In order to describe a curve, Lowe [4] chooses points in such a way that the density of retained points in an area is as high as the curvature is low in this area. Shape information is concentrated in the regions where the tangent is irregular.

All these methods are based on curvature measurements, which is a continuous concept. As Fischler and Bolles [5], we believe that a digital curve analysis requires discrete measures instead of discrete approximations of continuous measures. For example, derivatives are computed using a gaussian kernel convolution. This can correspond the continuous definition only if the smoothing parameter σ is large enough to be consider the pixel size as negligible. This implies that all small structures, although they are understandable for a human eye, are totally erased. Fischler and Bolles propose a discrete definition of critical point which is based on a study of a chord moved along the curve. A point will be declared as

- belonging to a smooth section if the curve stays close to the chord;
- critical if the curve makes a single excursion away from the chord;
- noisy if the curve makes multiple excursions away from the chord.

We propose in this paper a measure which is based on the comparison between chords lengths at different scales. As our approach is motivated by fractal considerations, we first present the common way to compute the fractal dimension, and show how the fractal approach does not allow an analysis of small structures. Then we define our measure, that we call k-regularity, and which depends on a scale parameter s and on a smoothing parameter k. In order to show the pertinence of the measure, we study its statistical behavior on two models of curves: the Brownian Motion and the digitized straight line. We present an application to image segmentation. The regularity measure is applied to frontiers and is used as a merging criterion in a region-growing algorithm. We show

experimental results obtained on an indoor image and on an aerial image, for which the interesting objects are man-made and thus are highly regular.

2 The Regularity Measure

Fractal theory introduces a nice notion of curve regularity with the fractal dimension [6], which describes the evolution of curve length as length measurement takes more and more details into account. To compute the fractal dimension of a curve, one typically processes the two steps:

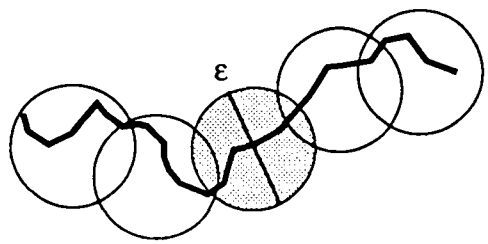

Figure 1: covering a curve with balls - $N(\varepsilon) = 5$

- for each value of a *scale* parameter ε, find how many balls of diameter ε are needed at least to cover the curve. In figure 1, we show an example where five balls are necessary to cover the curve for a given ε. Call $N(\varepsilon)$ that minimum number of balls.
- then estimate the limit slope of the function $-ln\varepsilon \mapsto lnN(\varepsilon)$ as ε tends to 0. This limit slope d is the fractal dimension of the curve.

Let us take an example with a generalization of the Von Koch curve. To build a Von Koch curve [7], take a segment of length 1, divide it in three segments of length 1/3 and replace the middle one by two new segments of the same length 1/3, in such a way that the resulting curve is a collection of 4 adjacent segments; then recursively apply this process to each of these 4 segments. In figure 2, we generalize the construction so that the length of the 4 segments is an arbitrary number $1/2 \geq \alpha \geq 1/4$.

For $\varepsilon_n = \alpha^n$, one needs $N(\varepsilon_n) = 4^n$ balls of diameter ε_n to cover the curve, so that $lnN(\varepsilon_n) = \dfrac{ln4}{ln\alpha} \cdot ln\varepsilon_n$. The fractal dimension is thus $d = -ln4/ln\alpha$. It varies from 1 when $\alpha = 1/2$ - the curve is then a straight line - to 2 when $\alpha = 1/4$ - the curve is then so agitated that it behaves more like a surface than like a curve. The Von Koch curve is obtained when $\alpha = 1/3$, and gives a fractal dimension of $ln4/ln3$.

In fact, the fractal dimension for a general planar curve belongs to the interval $[1 \ldots 2]$. The generalized Von Koch curve family take thus all possible values of the fractal dimension. From a visual point of view, curves of high fractal dimension are more agitated than

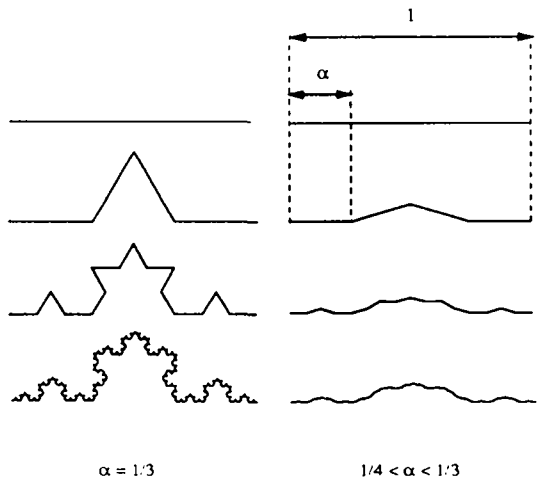

Figure 2: A generalization of the Von Koch curve.

curves of low fractal dimension. The more the fractal dimension is close to 2, the more the curve as a spatial extension that makes it behave like a surface. Note that the fractal dimension measures a microscopic behavior of the curve: if we stop the construction of the Voch Koch curve at a given depth of recursion, the fractal dimension is 1. Note also that in this example, the function $-ln\varepsilon \mapsto lnN(\varepsilon)$ is very well approximated by a straight line $lnN(\varepsilon) = ln1 - d \cdot ln\varepsilon$. This reflects the *self-similarity* of the curve: if we look at a part of the curve, we find a smaller copy of itself.

In a computer-vision framework, a curve is not continuous, but is a digitization of an underlying continuous curve. It is a finite set of connected pixels. For a fractal analysis, the scale parameter ε cannot be lower than one pixel, so that the fractal dimension computation must be modified as follows:

- for $\varepsilon = 1 \ldots k$ pixels, find how many balls $N(\varepsilon)$ are needed at least to cover the curve.
- then approximate the function $-ln\varepsilon \mapsto lnN(\varepsilon)$ by an affine function $lnN(\varepsilon) = lnL - d \cdot ln\varepsilon$ (figure 3) . The slope d is the fractal dimension of the curve.

For this process to reflect a fractal property, k must be large enough so that the lowest scale $\varepsilon = 1$ can be considered as a microscopic scale. In other terms, 1 must be negligible compared to k. While in the continuous case, fractal dimension is specific of a limit behavior at scale 0, the fractal dimension of a digitized curve takes into account informations on a scale range, from the microscopic scale, up to a macroscopic scale.

As image processing occurs in a discrete world where the pixel size may be not considered as negligible compared to the size of the objects represented in the image, we think it is necessary to find out a discrete definition of regularity which enables us to study the curve properties at low scales. We want to be able to extract the information which is

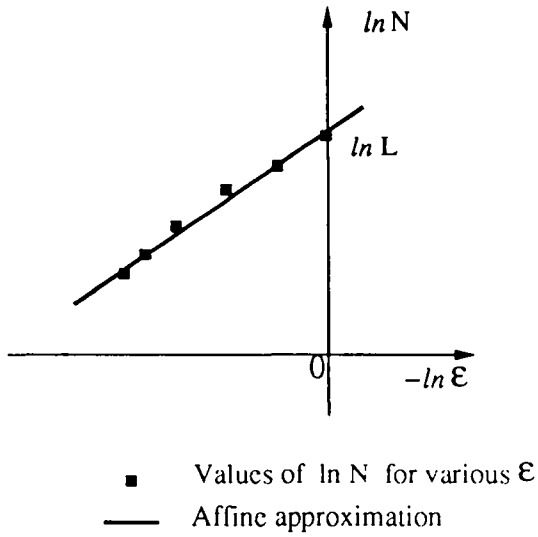

Figure 3: $lnN(\varepsilon) = lnL - d \cdot ln\varepsilon$ approximation

specific of a scale, and not of a scale range, even if that scale is very close to the pixel size. We propose here to see what information can be deduced of the comparison of lengths at two scales. We have chosen to see the scale parameter not as the diameter of a ball, but as an curvilinear length on the curve. This leads to a simpler definition. Lengths at two scales s and s' are comparable only if s' can be divided by s: $s' = k \cdot s$. So we have taken the following definition of comparison between lengths, that we have called *k-regularity*:

Definition: $R_{s,k}(C)$

Let $C = (P_i)_{i=1}^n$ be a digitized curve. The k-regularity at scale s of the curve C is defined as:

$$R_{s,k}(C) = \overline{r_{s,k}(C)(i)}$$

where:

$$r_{s,k}(C)(i) = \frac{\| p_{i+ks} - p_i \|}{\sum_{j=1}^{k} \| p_{i+js} - p_{i+(j-1)s} \|}$$

$R_{s,k}(C)$ is the mean value of $r_{s,k}(C)(i)$ along C. We can see k as a smoothing parameter.

Let us present the behavior of the k-regularity on two particular digitized curves: the Brownian Motion and the digitized straight line. These are our models of random irregularity and extreme regularity. The brownian motion is a curve where each point p_{i+1} has the same probability 1/4 to be one of four points connected to p_i, while the digitized straight line is the digitization of an underlying continuous straight line, where the position p_{i+1} is highly constrained by the positions of $p_{k \leq i}$. We have calculated the

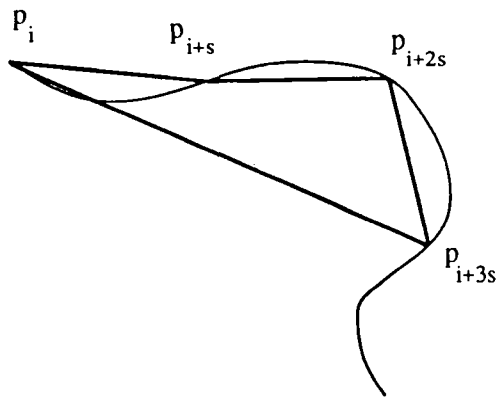

$$r_{s,k}(i) = \frac{\| p_{i+ks} - p_i \|}{\sum_j \| p_{i+js+s} - p_{i+js} \|}$$

Figure 4: $r_{s,3}$ at point i

means and variances for the k-regularity applied to these two curves, for different values of the scale parameter s and the smoothing parameter k. The values we present in figure 8 are calculated from an exhaustive exploration of the probability spaces.

For the Brownian Motion, the probability distribution of the vector $p_{i+k} - p_i$ does not depend on i [7], and the probability of the vector $p_{k+1} - p_1$ to be $(2i - k, 2j - k)$ is:

$$P = \frac{C_k^i \times C_k^j}{2^{2k}}$$

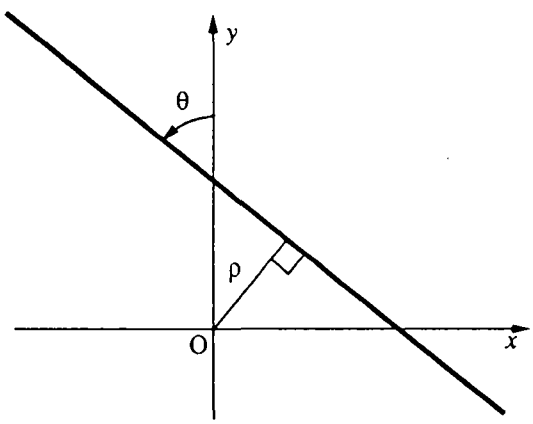

Figure 5: Line parametrization

For the digitized line, we have to compute the probability of a given set of pixels to be the digitization of a line. Following [8], the good parametrization for lines under reasonable invariance constraints is (ρ, θ): a line as the coordinates (ρ, θ) if it is at a distance ρ of the origin, and makes an angle θ with the y-axis (see figure 5). Lines are considered as following a uniform probability law if and only if ρ and θ follow a uniform probability law. So what we have to do is to compute for a given digitized curve, the surface in the (ρ, θ) space of the set of lines that may have produced that curve by a digitization process. In order to reach that goal, we need the following result:

Proposition:

Let A, B, C, D be four points in the plane, such that (A,B,C,D) is a convex polygone. Then the surface in the (ρ, θ) space of the set of lines that intersect the two segments (AB) and (CD) is:

$$S = AD + BC - AC - BD$$

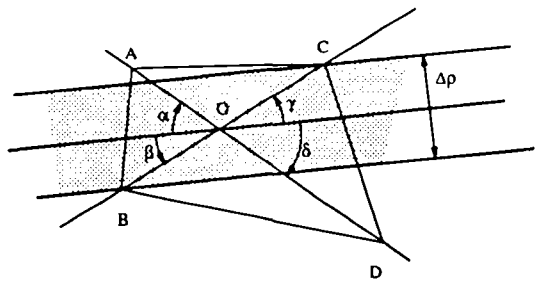

Figure 6: Lines in a given direction intersecting (AB) and (CD)

Proof:

Let $\Delta\Omega$ be the set of all lines intersecting (AB) and (CD). We want to calculate:

$$S = \int_{\Delta\Omega} d\rho d\theta$$

For a given value of θ, let:

- *O be the intersection between the lines (AD) and (BC).*
- *α, β, γ and δ be the angles between any line of direction ρ and the lines (AD) and (BC) as show in figure 6.*
- *$\Delta\rho$ be the partial sum $\int_{(\rho,\theta)\in\Delta\Omega} d\rho$*

We have:

$$\Delta\rho = \min(OA\sin\alpha, OC\sin\gamma) + \min(OB\sin\beta, OD\sin\delta)$$

When α is lower than the angle between (AC) and (AD), then $OA\sin\alpha$ is lower than $OC\sin\gamma$; otherwise, γ is lower than angle between (CB) and (CA), and $OC\sin\gamma$ is

lower than $OA\sin\alpha$. *So the integral on* θ *of the first term in* $\Delta\rho$ *can be rewritten* $OA - OA\cos(AC, AD) + OD - OD\cos(CA, CB)$ *or* $AD - AC$. *The same considerations on the second term in* $\Delta\rho$ *lead to the final result:*

$$S = \int \Delta\rho d\theta = AB + BC - AC - BD$$

□

In fact, the condition for a line to be digitized in a given discrete curve can always be expressed in such a way. Figure 7 shows the points A, B, C and D one can take in two examples of digitized lines.

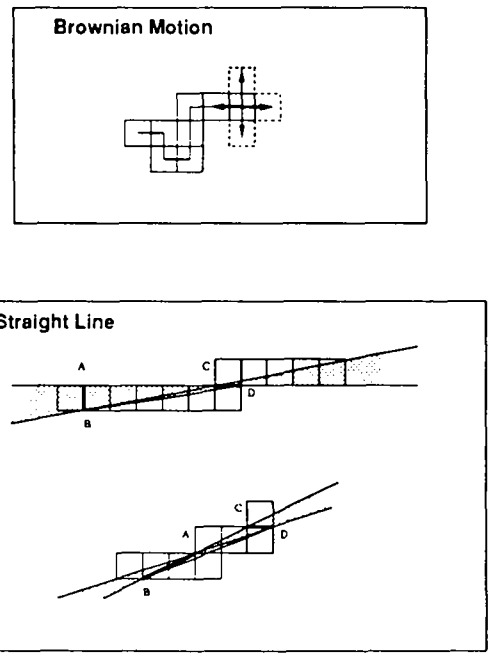

Figure 7: Underlying continuous lines for two digitized lines

Means or variances take then the expression:

$$E(f) = \frac{\Sigma_{\omega\in\Omega} S(\omega) \times f(\omega)}{S(\Omega)}$$

where Ω is the set of the digitized lines, $S(\omega)$ is the surface in the (ρ, θ) plane of the set of continuous lines that are digitized in ω, and f the function we want to calculate $(R_{s,k}, R^2_{s,k})$.

Let us analize the results of figure 8 and figure 9. Even when s and k are unreasonably close to the pixel size, $R_{s,k}$ reveals a pertinent information on the curve structure.

		Brownian Motion		Straight Line	
k	s	Mean	Variance	Mean	Variance
2	1	0.6036	0.1357	0.8284	0.0209
	2	0.7937	0.0925	0.9628	0.0015
	3	0.6732	0.0870	0.9810	0.0006
	4	0.7504	0.0853	0.9892	0.0001
3	1	0.5295	0.0530	0.8055	0.0117
	2	0.6455	0.0965	0.9547	0.0011
	3	0.5634	0.0553	0.9774	0.0004
	4	0.6053	0.0770	0.9871	0.0002
4	1	0.4383	0.0579	0.7967	0.0094
	2	0.5497	0.0795	0.9518	0.0009
	3	0.4828	0.0514	0.9762	0.0003
	4	0.5187	0.0616	0.9864	0.0001
5	1	0.4039	0.0369	0.7926	0.0084
	2	0.4852	0.0637	0.9505	0.0007
	3	0.4349	0.0407	0.9756	0.0003
	4	0.4611	0.0504	0.9860	0.0003

Figure 8: $R_{s,k}$ - Brownian Motion vs. Straight Line

Although variance is quite important, the line regular structure is visible even through $R_{1,2}$, which should *a priori* reflect nothing but a digitization noise. Of course, as s and k increase, the digitization effects are less and less important, so that $R_{s,k}$ discriminates more and more between the line and the random path.

So $R_{s,k}$ is a tool which is able to compute regularity at an arbitrary scale, even when the scale is very close to the pixel size. Let us see with the next section an application for which a close-to-the-pixel analysis is extremely useful.

3 An application to image segmentation

A region of a digitized image has two different signatures: the radiometric one depends on the pixel intensity inside the region, and the geometric one depends only on the line in $\mathbb{N}^2$ that is the region boundary. Numerous papers deal with segmentation based on radiometric models, and these models have been studied for a long time [9, 10, 11, 12, 13]. Authors [14, 15] have also studied the introduction of geometric models in the segmentation process. They consider the geometric analysis as a balance to the radiometric analysis. Formalizing the segmentation problem as an energy minimization problem, this leads to *minimize* an energy which takes the form $E = R + \lambda G$, where R computes the current partition radiometric deviation from the expected segmentation, and G the geometric one. The geometric factor, if used alone, leads to the trivial segmentation, where

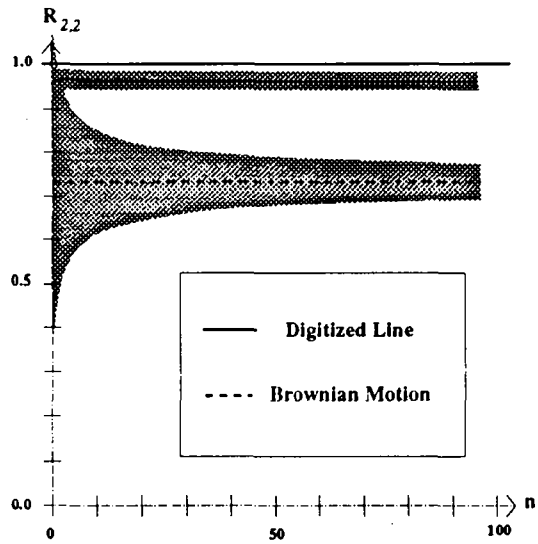

Figure 9: Standard deviation when curve length increases

the whole image is a single region. For Leclerc [14], the geometric part computes the length of the region boundaries. Fua and Hanson [15] propose more sophisticated criteria, each one dedicated to segment a particular class of objects. For example, the geometric part of a criterion devoted to find buildings out of aerial images takes the form:

$$G = \alpha\theta + \frac{2L}{s}$$

where α is a constant parameter, θ is the average deviation from $\pi/2$ multiples of the angle formed by the contour tangent and an fixed direction, L is the contour length and s is a scale parameter. So the energy's geometric part is minimum when regions boundaries are composed of segments in two orthogonal directions.

Pure geometrics models occur mainly in shape analysis, where objects boundaries are considered as already defined and when the segmentation process is over [2, 3, 4]. Our regularity measure may be used without being mixed to any radiometric criterion. Before we show how it is possible, let us explain why it is difficult to base a segmentation process on a pure geometric criterion. Following Zucker [13], a segmentation of an image X depends on a boolean predicate P, and consists of a set of X-subsets $\{X_i\}_1^N$ such that:

(i) $\{X_i\}_1^N$ is a partition of X.

(ii) X_i is connected.

(iii) $P(X_i)$ = TRUE for each i.

(iv) $P(X_i \bigcup X_j)$ = FALSE for $i \neq j$, where X_i and X_j are adjacent.

The predicate P determines whether a subset X_i is a part of a scene object or not. We can interpret (iii) as "each region belongs to at most one object", and (iv) as "each object contains at most one region". An algorithm can be naturally deduced from these points: from an original *over-segmentation*, that is a partition such that $P(X_i) = \text{TRUE}$ for each i, loop while possible:

$$\text{if } \exists (i,j), P(X_i \bigcup X_j) = \text{TRUE}, \text{then merge } X_i \text{ and } X_j$$

Let us take a simple example. Suppose we have to segment an image composed by two perfectly homogeneous objects: a black square on a white background. A "good" predicate would be:

$$P(X_i) : \int_{X_i} |I(x) - \bar{I}| dX_i = 0$$

The algorithm applied on any over-segmentation of X will lead to the true segmentation. But can we now imagine a pure geometric predicate that will lead to the true segmentation, whatever the original over-segmentation is? Can we geometrically decide whether a region belongs to a single scene object or not ? It is clear that the regions geometry is highly dependent on the initial over-segmentation. A region of the over-segmentation can have any arbitrary shape, so that the answer of the last two questions is NO, there is no over-segmentation independent geometric criterion which can lead to the perfect segmentation. Thus, if one wants to perform segmentation according to a geometric criterion, one must whether combine it with a radiometric one, in a $R + \lambda G$ style for example, or restrain the set of over-segmentation to a particular class, a class of *admissible partitions*. In this paper, we have chosen the latter solution, in order to show the effects of our regularity measure only. We have constrained the over-segmentation to be grey-level subsamplings. Figure 10 presents such an over-segmentation for an indoor image. Let us show now that the regularity measure is able to perform the segmentation as soon as the initial partition is a grey-level subsampling.

Regions boundaries in this kind of partition can belong to one of the two following classes:

- the region boundary is also an scene object boundary. In this case, the region boundary inherits the geometric regularity of the object boundary. We call this class *geometric boundaries*.
- the region boundary is *not* an scene object boundary. Here, the region is stopped *arbitrary*, depending on its texture or surface noise. We call this class *textural boundaries*.

Textural boundaries are irregular according to a close-to-the-pixel analysis, while geometric boundaries are regular. Our regularity measure should thus be able to distinguish the two classes of boundaries: textural boundaries are less regular than a certain threshold, geometric boundaries are more regular than this threshold.

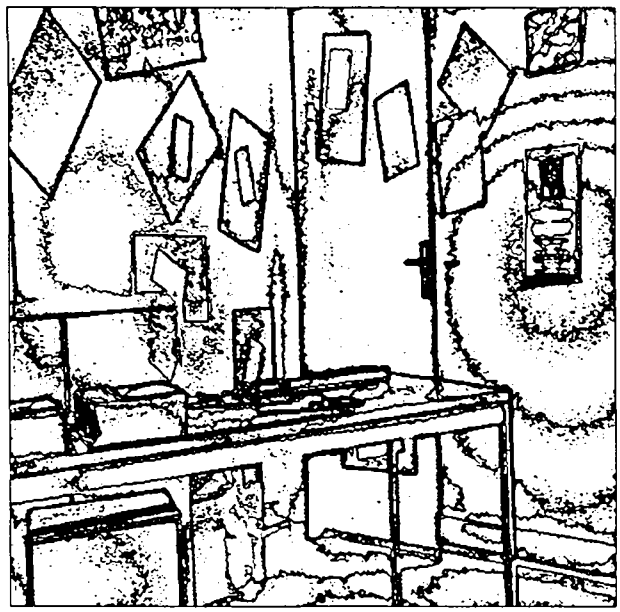

Figure 10: intensity subsampling

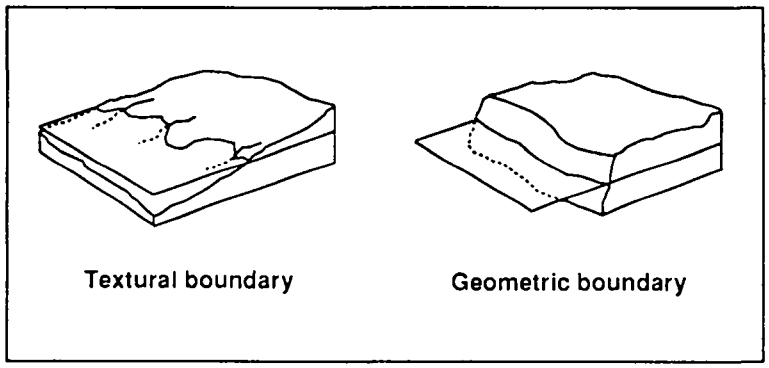

Figure 11: The two classes

4 Experimental Results

We have involved our regularity measure in a region-growing algorithm. Since we are interested in the close-to-the-pixel behavior of the curves, we have chosen $R_{2,2}$ to discriminate textural boundaries from geometric boundaries. We have fixed the threshold value to 0.92, which is a numeric approximation of the minimum regularity of the straight line. That means that the straight line is our model of regularity. The algorithm is inspired by the *sub-optimal segmentation algorithm* proposed by Monga [16]. The problem is that the formalism used by Monga, which follows the one presented by Zucker in [13], is not strictly applicable to a segmentation based on geometric criteria. Recall that a segmentation of an image X following a boolean predicate P should be a set of regions $\{X_i\}_1^N$ that is constraint by the four properties ((i) to (iv)) exposed in section 3. The choice of

same predicate P to determine whether a subset of X belongs to a single region or not, and to determine whether two subsets of X should merge or not, disables the possibility of using pure geometric predicates. To be more precise, each predicate that takes care only of what happens at the border of a subset is prohibited. In our case, two distinct objects may be merged, even if our criterion has decided that they were actually distinct.

These considerations lead us to adopt the following formalism:

(i) $\{X_i\}_1^N$ is a partition of X.

(ii) X_i is connected.

(iii) $P_r(X_i) = \text{TRUE}$ for each i.

(iv) $P_m(X_i, X_j) = \text{FALSE}$ for $i \neq j$, where X_i and X_j are adjacent.

We have to use two different predicates, a region predicate P_r which tests the ability of a subset to belong to a single object, and a merging predicate P_m which tests whether two subsets can belong to the same object or not. $P_m(X_i, X_j)$ must be FALSE if $P_r(X_i \bigcup X_j)$ is. For example, if we want to process a segmentation according to the regularity criterion, P_r would always be TRUE, and $P_m(X_i, X_j)$ would stand for: " the common frontier between X_i and X_j is a textural boundary". Note that one can choose $P_m(X_i, X_j) = P_r(X_i \bigcup X_j)$, in which case one come back to the Zucker formalism.

Monga proposes the use of a function that controls the *quality* of a segmentation. This function formalizes the *strategic* aspect of region growing. We use a function named $dQ(X_i, X_j)$ which quantifies the quality increasing of the segmentation when merging X_i and X_j.

Given an initial segmentation, the algorithm loops while possible on the three following points:

- determine the merging list, i.e. the list of P_m-mixable adjacent pair of subsets;
- sort the merging list according to dQ;
- merge the best independent pairs.

We present now the application of the algorithm on several grey-level images. Beginning with an intensity sub-sampled image, segmentation is performed in two steps:

- small regions merging: small regions cannot be efficiently treated by the regularity criterion, since their boundaries contain a very poor geometric information. At this step, $P_m(X_i, X_j)$ is TRUE if the length of the boundary of X_i is less than N pixels, where N has been arbitrary fixed to 10. $P_r(X_i)$ is always TRUE, and $dQ(X_i, X_j)$ increases as the average gradient along the common frontier decreases. Since the best *independent* pairs merge, a small region merge with exactly one of its neighbors.

- regularity merging: $P_m(X_i, X_j)$ is TRUE if the regularity $R_{2,2}$ of the common frontier is lower than a regularity threshold. The threshold's value is 0.92, as discussed previously. $P_r(X_i)$ is TRUE whatever X_i is, and $dQ(X_i, X_j)$ is equal to $P_m(X_i, X_j)$.

In the following figures, the upper-left image (A) is the grey-level image, the upper-right image (B) is the grey-level subsampling, the lower-left image (C) is obtained from (B) by removing small regions, and the lower-right image (D) is obtained from (C) by applying the regularity merging.

Figure 12 shows the segmentation processing on an indoor image. This first result shows our regularity criterion's ability to detect irregularity in a practical case. One can see that each irregular boundary in image (C) has been removed in image (D). Some other boundaries seem to have also disappear, in the poster on the right wall for example. In fact, this is not the case. Merging occurs here because there are regions of the intensity subsampling which belong to both the poster and the wall. These regions present irregularity against the wall, and irregularity against the poster, so that the poster is finally merged to the wall. This kind of problem is actually due to an incompatibility between our definition of acceptable partitions and the definition of over-segmentation (see section 2).

Figure 13 shows the segmentation processing on the aerial image an airport. The airport shows another direct application of the method described in this paper. Main structures have been correctly segmented, but some objects such as the group of trees on the upper-left corner have disappeared. This is due to the simplicity of the strategic function dQ we have used. Better results are obtained with the same merging predicate, but with more sophisticated strategic functions which quantify a confidence we can have in the regularity measure.

The grey-level subsampling of the image shown in figure 14 leads to numerous small regions. In that case, the common frontier between two regions is almost everywhere only a few pixels long. Their geometric quality is thus so poor that the geometric criterion fails in many cases to discriminate correctly between geometric and textural edges. But the overall quality of the final segmentation reflects the image's main structures such as the town, the lake, and the roads. One can remark in particular that almost all the frontiers between fields and roads are preserved.

5 Conclusions

We have presented in this paper a set of geometric measures that quantify regularity of digitized curves. These measures have been theoretically tested on models of irregular and regular curves, the Brownian Motion and the digitized straight line. One of our regularity measure has been involved in a region-growing segmentation algorithm, and has shown its practical ability to perform segmentation on images where interesting features are man-made objects. In this paper, we have only use the regularity criterion as the decisive criterion. But it is possible to have it cooperate with other criteria, and in particular with radiometric criteria. Cooperation with radiometry may occur in two ways:

- the strategic function decides which mergings should come first;
- the initial radiometric over-segmentation gives its input data to the geometric criterion;

We have found two limitations on the use of the regularity measure. The first one is that the regularity measure takes a practical sense only if the length of the curve is large enough compared to the scale parameter. Our current work is to precise the confidence one can have in the regularity measure, depending on the length of the analized curve. The second one is that in the segmentation process we propose, the initial segmentation is highly constrained by the fact it must be an admissibility partition, so that a few radiometric criteria can be used here. In some cases, the admissibility criterion may be in conflict with the over-segmentation criterion. We have to find now is another and larger class of admissible partitions which eliminates that contradiction. One possible way is admissible frontiers instead of admissible partitions. The admissible frontiers would be the only frontiers to be allowed to disappear in a region merging. This would lead to a larger class of geometric-unstable over-segmentations, and would allow many radiometric criteria to be used in the presegmentation process.

References

[1] Rogowitz and Voss, "Shape Perception and Low-Dimension Fractal Boundary Contours". Research Report, IBM Research Division, July 16, 1990.

[2] Mokhtarian and Mackworth, "A Theory of Multiscale, Curvature-Based Shape Representation for Planar Curves". IEEE Transactions on Pattern Analysis and Machine Intelligence, Vol. 14, n°8, p. 789-805, August 1992.

[3] Asada and Brady, "The Curvature Primal Sketch", IEEE Transactions on Pattern Analysis and Machine Intelligence, Vol. PAMI-8, n°1, p. 2-14, January 1986.

[4] Lowe, "Organization of Smooth Image Curves at Multiple Scales". International Journal of Computer Vision, 3, p. 119-130, 1989.

[5] Fischler and Bolles, "Perceptual Organization and Curve Partitioning", IEEE Transactions on Pattern Analysis and Machine Intelligence, Vol. PAMI-8, n°1, p. 100-105, January 1986.

[6] Mandelbrot, "The Fractal Geometry of Nature", Freeman, San Francisco, 1982.

[7] Falconer, "Fractal Geometry, Mathematical Foundations and Applications". *John Wiley and Sons Ed.*, p. xiv-xv and p. 238-241, 1990.

[8] Santalo, "Integral geometry and geometric probability". Cambridge university press, 1984.

[9] Pavlidis, "Segmentation of Pictures and Maps through Functional Approximation". *Computer Graphics and Image Processing*, 1, p. 360-372, 1972.

[10] Brice and Fennema, "Scene Analysis using regions". *Artificial Intelligence*, 1, p. 205-226, 1970.

[11] Horowitz et Pavlidis, "Picture Segmentation by a directed Split and Merge Algorithm". *Proc. Second Int. Joint Conf. Pattern Recognition*, 1974.

[12] Feldman and Yatimovsky, "Decision Theory and Artificial Intelligence, I. A Semantics-Based Region Analyzer". *Artificial Intelligence*, 5, p.349-371, 1974.

[13] Zucker, "Survey Region Growing: Childhood and Adolescence". *CGIP*, n°5, p. 382-399, 1976.

[14] Leclerc, "Constructing Simple Stable Descriptions for Image Partitioning". *International Journal of Computer Vision*, 3, p. 73-102, 1989.

[15] Fua and Hanson, "Extracting Features from Aerial Imagery Using Model-Based Objective Functions". Artificial Intelligence Center, Computer and Information Sciences Division, SRI International, October 22, 1988.

[16] Monga and Wrobel, "Segmentation d'images: vers une méthodologie". *Traitement du Signal*, 4, n°3, p. 169-193, 1987.

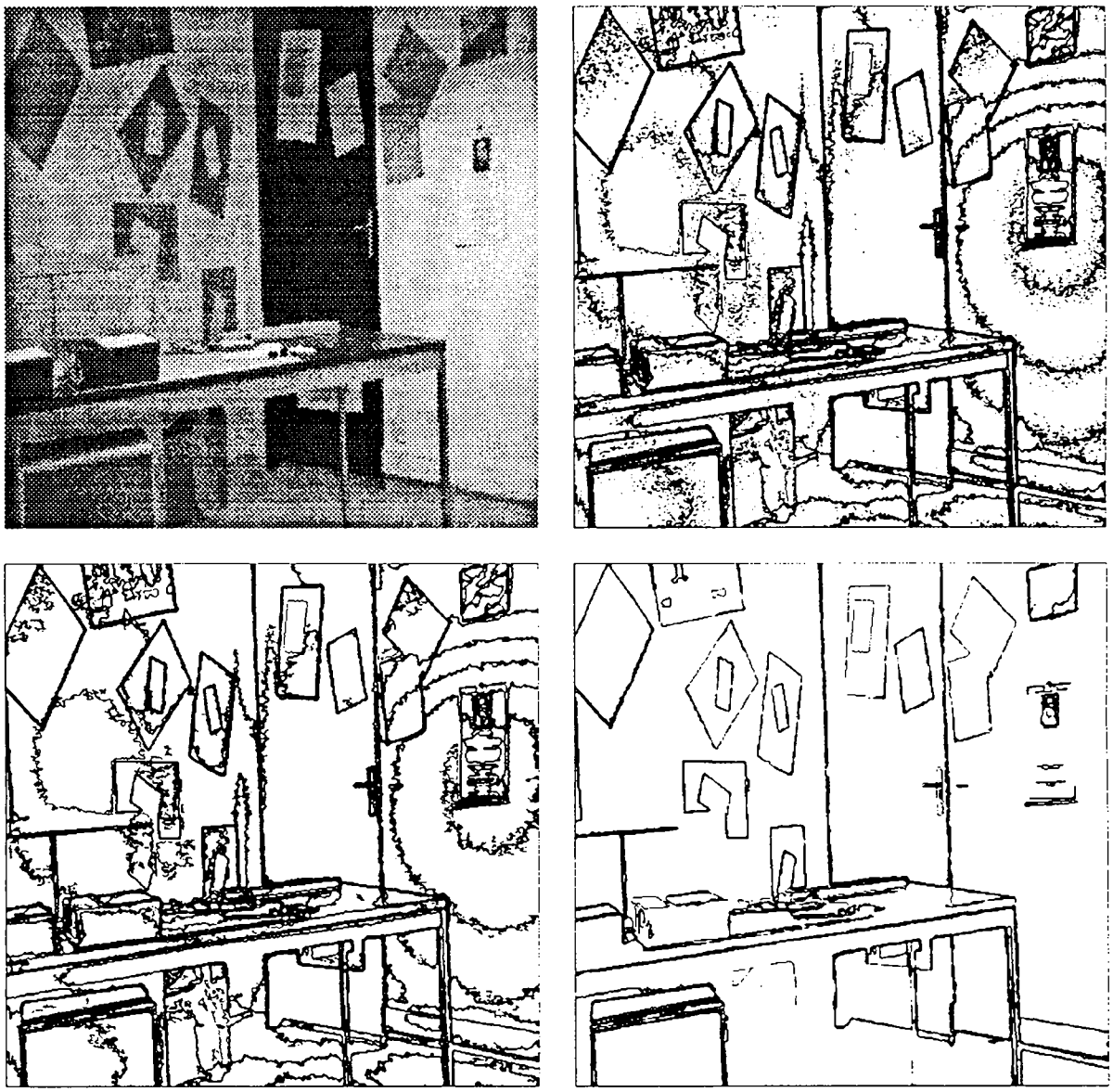

Figure 12: indoor processing

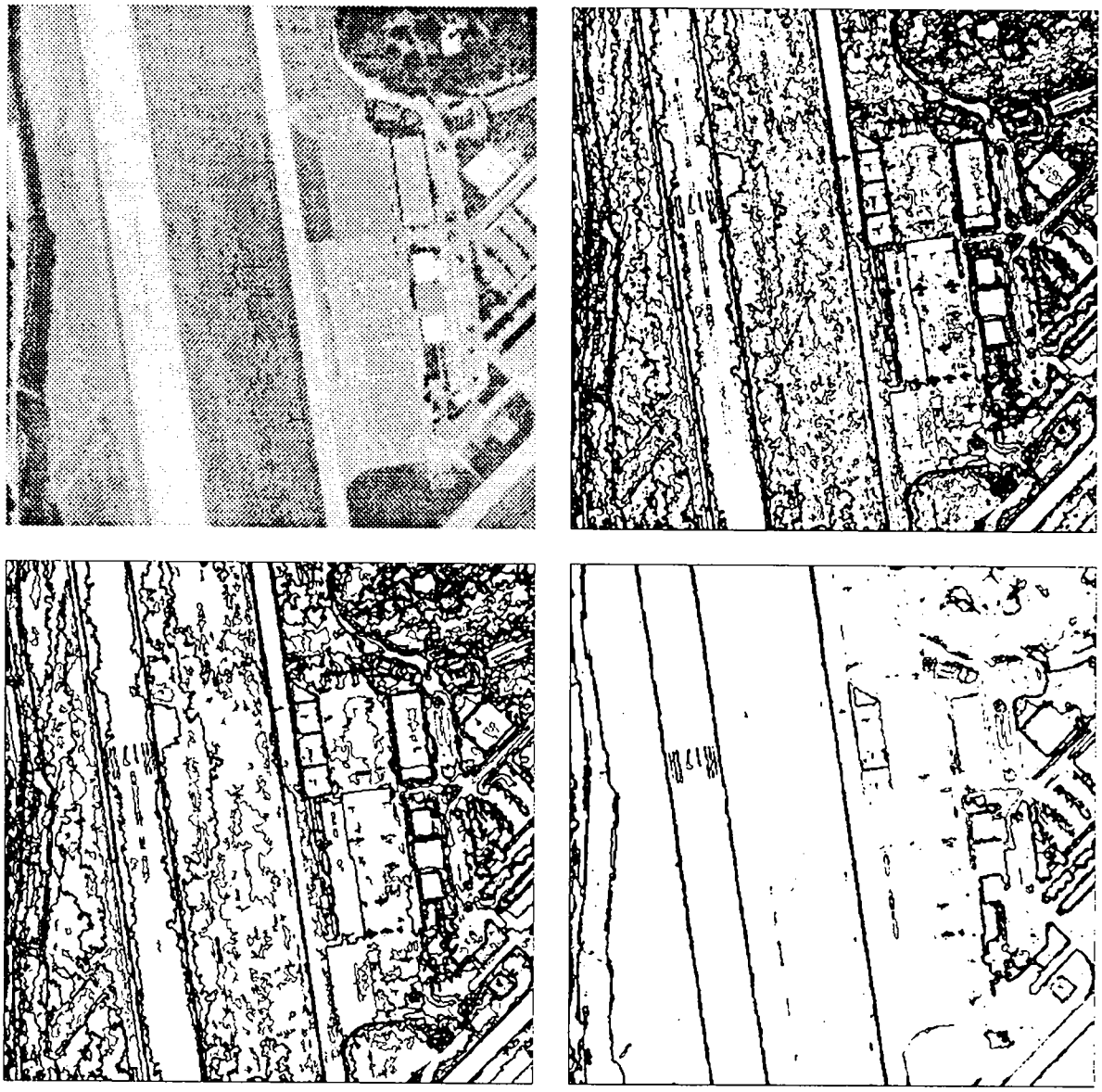

Figure 13: airport processing

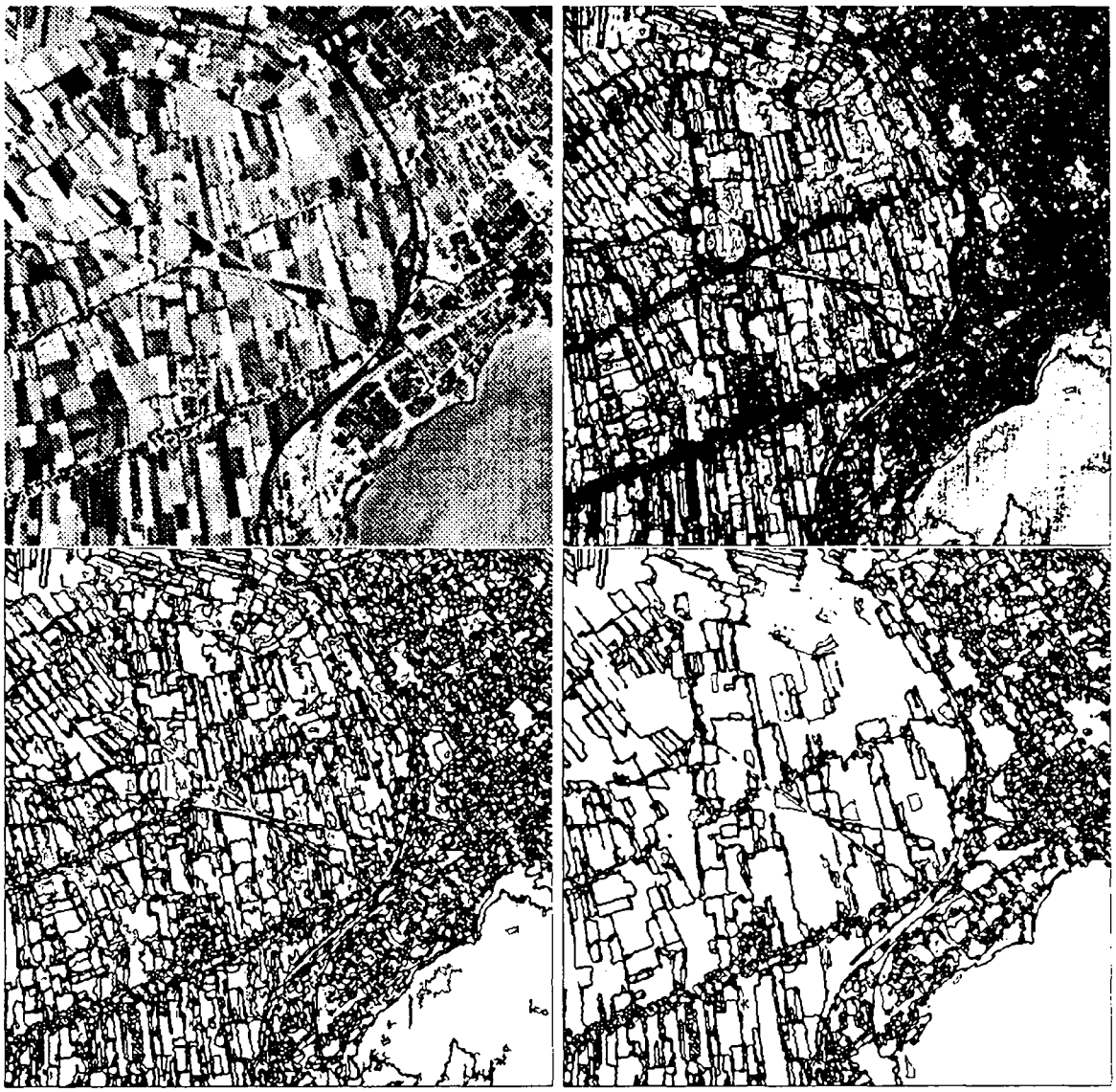

Figure 14: fields, lake and town

Unité de Recherche INRIA Sophia Antipolis
2004, route des Lucioles - B.P. 93 - 06902 SOPHIA ANTIPOLIS Cedex (France)

Unité de Recherche INRIA Lorraine Technopôle de Nancy-Brabois - Campus Scientifique
615, rue du Jardin Botanique - B.P. 101 - 54602 VILLERS LES NANCY Cedex (France)
Unité de Recherche INRIA Rennes IRISA, Campus Universitaire de Beaulieu 35042 RENNES Cedex (France)
Unité de Recherche INRIA Rhône-Alpes 46, avenue Félix Viallet - 38031 GRENOBLE Cedex (France)
Unité de Recherche INRIA Rocquencourt Domaine de Voluceau - Rocquencourt - B.P. 105 - 78153 LE CHESNAY Cedex (France)

EDITEUR
INRIA - Domaine de Voluceau - Rocquencourt - B.P. 105 - 78153 LE CHESNAY Cedex (France)

ISSN 0249 - 6399